PEARL: the high pressure neutron powder diffractometer at ISIS

C. L. Bull, N. P. Funnell, M. G. Tucker, S. Hull, D. J. Francis and W. G. Marshall

Published version information

Citation: Bull, CL et al. "PEARL: the high pressure neutron powder diffractometer at ISIS." High Pressure Research, vol. 36, no. 4 (2016): 493-511.

doi: https://doi.org/10.1080/08957959.2016.1214730

This is an Accepted Manuscript of an article published by Taylor & Francis in High Pressure Research on 05/08/2016, available online: https://doi.org/10.1080/08957959.2016.1214730

To appear in *High Pressure Research*
Vol. 00, No. 00, Month 20XX, 1–17
10.1080/0895795YYxxxxxxxx

PEARL: the high pressure neutron powder diffractometer at ISIS

C. L. Bull[a*], N. P. Funnell[a], M. G. Tucker[†a], S. Hull[a], D. J. Francis[a] and W. G. Marshall[a]

[a]*ISIS Facility, Rutherford Appleton Laboratory, Chilton, OXON, U.K.*

(*Received 00 Month 20XX; final version received 00 Month 20XX*)

The PEARL instrument at ISIS has been designed for, and dedicated to, in-situ studies of materials at high pressure, using the Paris–Edinburgh press. In recent years, upgrades to the instrument have led to improvements in data quality and the range of achievable pressures and temperatures; currently 0.5–28 GPa and 80–1400 K. This paper describes the technical characteristics of the instrument, its current capabilities, and gives a brief overview of the science that has been performed, using representative examples.

Keywords: neutron, diffraction, large volume press, high pressure, temperature, crystal structure

1. Introduction–neutron diffraction at high pressure

The advantages of neutron radiation in diffraction, compared to those of X-rays, have been well-documented, as has the role of high pressure in neutron diffraction experiments.[1, 2] In brief, neutrons interact with sample atoms in a different manner to X-rays; X-rays are scattered by the diffuse electron cloud, which gives rise to pronounced decay in the form factor with increasing scattering vector Q, whereas neutron scattering occurs at the atomic nucleus—a point scatterer—thus the form factor is independent of Q, resulting in high spatial resolution. The magnitude of the interaction at the nucleus is not directly proportional to the atomic number Z of the atom (unlike the X-ray experiment) and as a result, low-Z atoms do not inherently have small scattering lengths, e.g. deuterium atoms in water (D_2O) dominate its neutron diffraction pattern, in contrast (and also in complement) to the equivalent X-ray pattern, which sees oxygen as the stronger scatterer. Furthermore, the ability of neutrons to discriminate between atoms with similar Z permits study of mixed-site materials, e.g. perovskites. Neutrons have a high penetration depth in comparison to X-rays and so sample environments such as metal pressure cells can be accommodated. Lastly, as a result of their intrinsic spin, neutrons are sensitive to magnetic order within materials, allowing determination of their magnetic structure.

At the ISIS Pulsed Neutron and Muon Source, the first pressure experiments in the 1980's used piston cylinder and gas cell techniques.[2, 3] In the late 1980's, a collaborative effort between the Universities of Paris and Edinburgh led to the development of the

[†]Now at: Spallation Neutron Source, One Bethel Valley Road, MS-6475, Oak Ridge, TN, U.S.A.
[*]Corresponding author. Email: Craig.Bull@stfc.ac.uk

Paris–Edinburgh (PE) press—a lightweight press [4] equipped with Bridgman-type opposed anvils, with a toroidal profile, based upon an existing anvil design by Khvostantsev *et al.*[5] There is no technical way of getting around the fact that it is necessary to have small sample volumes in order to achieve high pressure conditions, however this presents difficulties when applied to neutron experiments, given the flux of neutrons is low compared to that of X-ray sources. Thus the typical sample volume of the PE press is a compromise between the need to obtain reasonable counting statistics whilst still attaining multi-GPa pressures. To-date, in a typical neutron experiment, the press is capable of generating up to ca. 30 GPa of pressure in a temperature regime ranging between 80–1400 K.[6] At ISIS, the V3 and V4 variants of the PE press are routinely in use (although other devices are available for specialist experiments), delivering up to 250 tonnes of force—further details of the press are documented elsewhere.[2]

PEARL—the dedicated high pressure neutron instrument at ISIS—was designed around the PE press and has, for the past 18 years, formed a significant part of the user programme at the ISIS facility. In 2010, the instrument was upgraded, replacing the existing array of detectors and installing a new low-angle bank. In this paper we describe the current capabilities of PEARL, provide some examples of the science performed, and offer an outlook for the future of the instrument, with a view to enhancing the user programme and the range of science possible. We also detail the infrastructure that has developed around the pressure cell. The overriding aim is to both further the field of high pressure science while providing non-specialist users the ability to use pressure as a powerful thermodynamic variable in their research.

2. The PEARL instrument

PEARL is a medium-resolution, high-flux instrument, located on beamline S9 of Target Station 1 at ISIS. The layout/geometry of PEARL is shown schematically in Figure 1 and technical data is presented in Table 1. The instrument is located such that it has an oblique view of a liquid methane moderator, which operates at 110 K. On leaving the moderator, the neutron beam is collimated using a pair of movable B_4C jaws, which define the beam size at the sample position—typically 5×5 mm. Before, after, and between the jaw sets are scintillation monitors based on the GS series of glass scintillators from Scintacor. The scintillator is alumina-silicate with ^{6}Li-enriched lithium oxide.[7] The monitors provide a measure of the neutron flux profile as a function of time-of flight (ToF) and quantify the effects of the jaws, often being used for instrument diagnosis purposes and normalisation within data reduction techniques. The centre of the PE press, and hence the sample, is situated 12.8 m from the moderator. The press is contained within an evacuated sample tank, which is supported by a metal frame that orients the press toward the incident neutron beam. The absolute position of the tank can be fine-tuned by a motorised sliding mechanism that translates it along the length of the beam path ensuring that the sample is always situated at the defined instrument centre (this is prone to change on pressurisation—described later). This means that the ToF path from moderator to sample is always maintained, producing correctly calibrated and comparable d-spacing values throughout an experiment.

The metal frame also supports two sets of detectors—the main, transverse, detectors are situated normal to the incident beam and are located 0.8 m from the sample position. The transverse detector bank is comprised of 9 modules, each containing 78 zinc sulfide scintillator elements, each spanning 3 mm within the $81.2^\circ \leq 2\theta \leq 98.82^\circ$ diffracting angles. This acceptance angle is defined by the opening angle of the toroidal profile of the anvils currently used in the PE press. For the standard ISIS 20 ms frame, the transverse

Table 1. PEARL instrument technical characteristics and capabilities. Refer to the mansuscipt text for further details and specific information.

Instrument Parameter	Value
ToF range (μs)	1500–20000
Useable d-spacing range (Å)	0.4–4.1, 12.5 (transverse, longitudinal)
2θ range—transverse (°)	$81.2 \leq 2\theta \leq 98.8$
2θ range—longitudinal (°)	$20.0 \leq 2\theta \leq 60.0$ & $100.0 \leq 2\theta \leq 160.0$
Wavelength range (Å)	0.4–5.8
Moderator to sample distance (m)	12.8
Sample to transverse detector distance (m)	0.8
Sample to longitudinal detector distance (m)	1.2
Transverse average resolution $\Delta d/d$ (%)	$\sim$0.64
Pressure range (GPa)	0.5–28
Temperature range (K)	80–1400

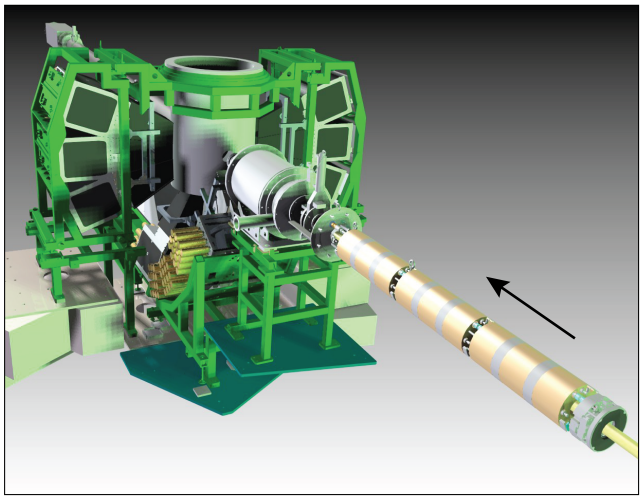

Figure 1. Schematic of the PEARL instrument. The incident beam arrives from the moderator on the lower-right hand side of the image, in the direction indicated by the arrow, passing through the beam pipe which also houses the jaw sets, monitors, and scrapers. The PE press sits in the sample tank at the centre of the instrument. Surrounding the sample position, perpendicular to the beam, are transverse detector banks. Also visible, are some of the low-angle banks, near the bottom of the figure. In normal use, all detectors are covered in polethylene shielding to reduce background levels in diffraction patterns.

detector bank is able to observe d-spacings in the approximate range 0.5–4.1 Å, with a nominal average resolution $\Delta d/d$ of ca. 0.64%. The readout from each pixel of the detector can be separated, and grouped by diffraction angle, permitting the study of micro-structure in, for example, textured ice samples.

The longitudinal detector bank consists of three modules covering the back-scattering angular range $100.0° \leq 2\theta \leq 160.0°$, and a forward-scattering low-angle bank of $20.0° \leq 2\theta \leq 60.0°$, where each module contains 78 zinc sulfide scintillators. These detector banks are accessed by rotating the cell by 90° and allows the incident and scattered beam to pass through the gasket. Each detector module is situated 1.2 m from the sample position and allows access to a maximum d-spacing of 12.5 Å, however this comes at the expense of significantly-reduced resolution. The pulsed nature of the neutron beam itself also provides a means to measure longer d-spacing. The pulse structure at ISIS delivers four out of five 20 ms pulses to Target Station 1, with the fifth going to the second ISIS Target Station, thus it is possible to continue counting the fourth pulse for up to 40 ms—the slower neutrons enable measurement of up to ca. 8 Å in the standard 90° transverse geometry. The caveat is that counting statistics are reduced, relative to the rest of the measured

powder pattern, given that i) only a quarter of the neutron pulses contain neutrons with the required energies, and ii) neutron flux at longer wavelengths is significantly reduced as a result of moderator performance (however, diffracted long-wavelength neutrons produce stronger Bragg reflections as peak intensity $\propto \lambda^4$). Nevertheless, this approach has been used with some success, particularly in aiding the indexing of new phases and investigation of magnetic reflections.

3. Performing an experiment on PEARL

In general, high pressure experiments on PEARL are performed routinely up to ca. 12 GPa—although pressures of ca. 28 GPa are attainable with user-supplied sintered diamond anvils—and current temperature capability ranges between 80–1400 K. The type and magnitude of thermodynamic parameters being explored dictates which variant of the PE press is used; a selection of V3, V4, V7 and VX3/4 PE presses are available (the differences and relative merits of these presses have been described elsewhere in detail [2, 8]). The same is true of the sample gasket and anvils—these are described in more detail in Section 4.

In the case of a 'standard' room-temperature experiment, a V3 PE press is typically used. The press is suspended on a flange and inserted inside a vacuum tank—see Figure 2—which is mounted within the steel frame detailed in Figure 1. All equipment is moved into the PEARL instrument by means of an overhead crane. An alignment camera, situated perpendicular to the cell, allows continuous optical access to the cell which, in combination with the frame translation mechanism, ensures the centre of the gasket remains at the calibration position throughout the experiment. This is essential as load is applied to the gasket by means of driving a piston towards one of the anvils, displacing the gasket away from the instrument centre, along the beam direction. The instrument is controlled by the in-house SECI (Sample Environment Control Interface) software, which is capable of running and monitoring the vacuum system, alignment motors, jaw sets, Eurotherm temperature controllers, data acquisition and the automated pressure system.

Hydraulic load can be applied to the PE press piston using either oil, pentane, or helium gas. In the case of oil or pentane, load increase/decrease can be controlled, maintained and fully automated (by means of scripting) through a pressure control system (Figure 2), which consists of a pair of stepper-motor-driven Capstan pumps. The upper hydraulic load limit of the automated system is 1 kbar, above which pressure must be controlled manually with a hand pump. For pressure cells driven by helium gas, a double-headed electrically-driven pump is available with a room-temperature buffer volume—the buffer ensures that a constant load is applied when the temperature of the cell is changed.

All measured data are reduced and visualised using the MANTID software package.[9] The basic reduction procedure starts by focussing and summing the individual detector spectra, normalises the summed pattern with respect to the incident beam monitor, and corrects for detector efficiency against a vanadium standard dataset, collected at the start of each user cycle. Finally, the software applies the effects of wavelength- and angle-dependent beam attenuation by the anvils. The data are outputted in a format suitable for a range of powder refinement packages, including GSAS, Fullprof and TOPAS Academic.[10–12]

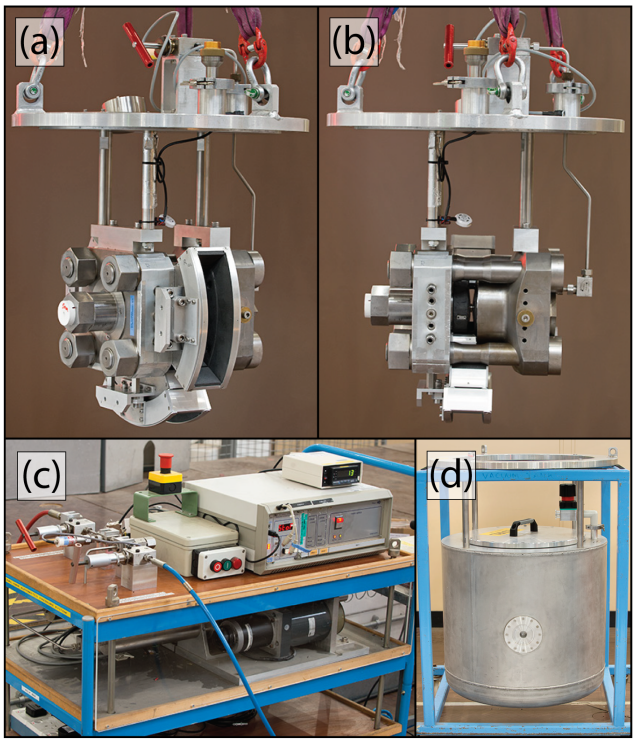

Figure 2. (a) V3 variant press. The incident beam passes from left to right and is initially collimated by a boron nitride (white) insert with a 5 mm hole in its centre, allowing the beam to pass through into the centre of the press. The diffracted beam leaves at 90° through the boron-coated collimation 'ears'. (b) Side view of the V3 press with right-hand collimator 'ear' removed; the gasket containing the sample is situated at the centre of the boron-coated anvils. To the right-hand side of the press is a hydraulic feed-through pipe that connects the piston to the automated pump system. (c) PC-controlled automated hydraulic load system—the load is increased/decreased by a stepper-motor system, which rotates a Capstan 1 kbar pump. The automated system can be used with oil or pentane. (d) Vacuum tank, which sits in the centre of the PEARL instrument (visible in Figure 1). The top flange of the PE press is supported by the top of the vacuum tank, suspending the cell in the centre.

4. Tailoring the PE press to the experiment—available options

4.1. *Anvils*

The common anvil geometry used on PEARL is that of the toroidal anvils, shown in Figure 3, where there is a central cup—based on the profiled Bridgman anvil—the dimensions of which define the maximum sample volume.[5, 13] The toroidal outer ring of the anvil, designed by Khovstantsev *et al.* accommodates the toroidal component of the gasket (described later) which supports the central part of the gasket against its internal hoop stresses by restricting its outward flow, increasing the attainable pressure.[14]

Three types of anvil material are generally used in transverse geometry experiments on PEARL: i) tungsten carbide (WC); ii) SD; and iii) zirconia-toughened alumina (ZTA)—images of each are shown in Figure 3. Historically, WC was the standard choice of anvil material due to its toughness, however it has some undesirable features, namely its marked attenuation of the neutron beam, and its relatively poor (by current standards) signal-to-background level—see Figure 3. Each of the anvils is supported by a fret made of hardened steel, radially supporting the anvil, which increases the maximum attainable pressure prior to anvil failure.[2] The upper pressure limit of the WC anvils is ca. 10 GPa.[4] SD anvils alleviate many of these issues, possessing fewer Bragg reflections (but strong Bragg edges), exhibiting a decreased level of background scattering and reduced attenuation of the beam, however these come at a significantly-increased monetary cost. With a single-toroidal profile, they will generate up to 12 GPa of pressure on the sample, but use of a

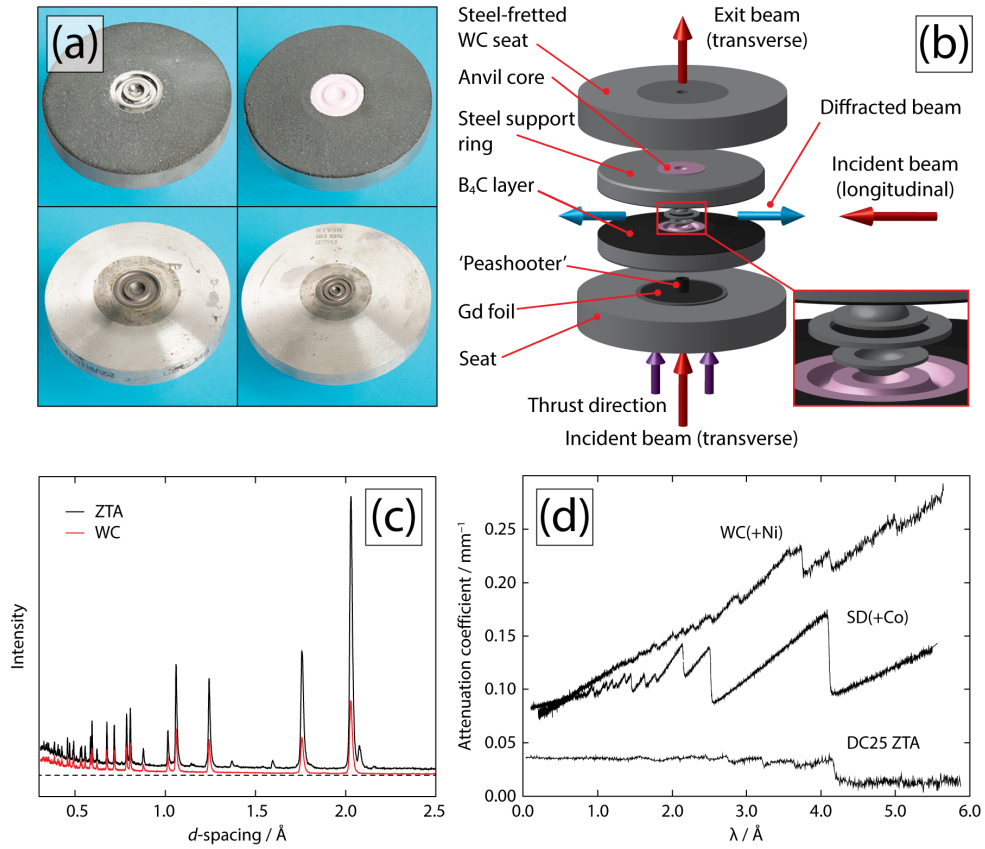

Figure 3. (a) From top-left, clockwise: single-toroidal WC, single-toroidal ZTA ceramic, double-toroidal SD, and single-toroidal SD anvils. The WC and ZTA anvils shown here are coated in boron for shielding. The anvils oppose the sample gasket, as shown in (b), and these in turn are sandwiched between steel-fretted WC seats, with gadolinium foil and a 'peashooter' tube. The direction of the incoming neutron beam depends on which detector banks are being used, but the diffracted beam always exits in the horizontal plane, with respect to the diagram orientation, indicated by the blue arrows. (c) The diffraction patterns of a nickel pellet, collected for the same amount of time in the PE press when equipped with ZTA and WC anvils—a marked improvement in scattering intensity is evident for the ZTA anvils. The dotted line indicates zero intensity—the y-axis is plotted to negative values for Figure clarity. (d) Attenuation coefficients of ZTA, WC and SD anvils as a function of wavelength. Beam attenuation is drastically reduced when the ZTA anvils are in use, as well as possessing less intense Bragg edges. The strongest attenuation, coupled with multiple complex sharp features is seen in the WC anvils, especially at longer wavelengths.

double-toroidal profile will, in principle, allow pressures of 28 GPa to be reached, although this maximum pressure is usually only achieved at the expense of the anvil integrity itself. Twenty gigapascal is a more routinely-used upper pressure limit as this allows recovery and reuse of the anvils. Images of single and double-toroidal anvils can be seen in Figure 3. These very high pressures demand a reduced sample volume, thus data collection times are increased if equivalent counting statistics are to be obtained—this is described in detail elsewhere.[6]

More recently, ceramic ZTA anvils have been developed with mechanical properties that are comparable to those of WC but possess the distinct advantage in their high neutron transparency—see Figure 3—and relatively low cost.[2] Their neutron transparency is still maintained at longer wavelengths; at 4 Å there is an order-of-magnitude improvement in diffracted signal over the other anvil types. This transparency is reduced with shorter wavelengths but is still significantly higher than that of the WC anvils—at 1 Å, ZTA and WC attenuation lengths are ca. 0.037 and 0.1 mm^{-1}, respectively, and at 4 Å, they measure ca. 0.01 and 0.2 mm^{-1}. They are suitable for repeated use in the 0–7 GPa regime, operating over the temperature range 80–500 K. Their general 'all-around' suitability has

made ZTA the standard anvil material of choice for the majority of experiments in the user programme.

An important consideration in anvil design is to reduce unwanted scattering by extraneous components of the anvil and frettage as far as possible. This is achieved through the use of shielding: covering the frets with either cadmium foil or, more recently, a B_4C epoxy mixture. On the reverse side of the anvil, a small sheet, and a 'peashooter' tube that extends into hole of the WC seat, of gadolinium foil, are often included to suppress scattering from the anvil, shown in Figure 3.

4.2. *Gaskets and hydrostatic media*

The majority of gaskets are machined from the null-scattering Ti–Zr alloy, composed of 67.6 mol% titanium and 32.4 mol% zirconium; elements which have negative and positive neutron scattering lengths, respectively. The constituent parts of the gasket are assembled to form a small sample chamber—shown in Figure 4—the standard gasket being an open disc, with a support ring, for use with solid materials under non-hydrostatic conditions. If a fluid sample, or hydrostatic conditions are required—which usually necessitate the presence of a pressure-transmitting fluid—then an encapsulated variant of the gasket [15] must be used as otherwise the fluid can penetrate the anvils, causing them to fail at pressures as low as ca. 4 GPa. Along with the sample and hydrostatic medium, a small pressure marker is included, allowing determination of pressure at the sample position. Subject to sample solubility and permeability, a perdeuterated methanol/ethanol mixture, in a 4:1 volume ratio, is usually the pressure-transmitting fluid of choice—this allows hydrostatic compression up to ca. 10.5 GPa.[16] It can be used to compress the sample beyond this pressure, still within a hydrostatic regime, but only when heated, keeping the temperature of the gasket above the freezing point of the methanol/ethanol mixture.[17]

Alternative commonly-used pressure-transmitting media are pentane/isopentane mixtures and Fluorinert, but these are limited to hydrostatic pressures of ca. 6 and 2.5 GPa respectively.[18] Perdeuterated pentane mixtures present additional difficulties because of their high volatility—these are best loaded into the gasket by cooling to 260 K on a chiller plate within a nitrogen-containing box (to prevent condensation of atmospheric water), both available in the PEARL sample preparation cabin. The nitrogen box can also be used for loading air-sensitive samples. Hydrostatic media are not restricted to just room-temperature liquids—argon gas can be used as a pressure-transmitting medium through one of two routes: i) cryogenically liquefying it into the gasket or ii) using a built-for-purpose gas loader; the latter method is performed routinely as part of the PEARL user programme. Details on both procedures are available elsewhere.[19–21] More recently a new gas loader designed by Klotz *et al* in which gases (including deuterium) are loaded into a clamp at 2 kbar gas pressure prior to insertion into the VX3 PE press, has become part of the user programme.[22]

4.3. *Attenuation corrections*

The complex sample environment leads to a non-trivial beam attenuation correction as the neutrons pass through several materials at various angles and path lengths, as well as possessing different wavelengths with varying 2θ, which also influences the correction.[23] As can be seen in Figure 3, the incident beam first passes through one of the anvils and the gasket, before reaching the sample and being diffracted. This diffracted beam then traverses through the remainder of the sample and gasket, in an approximately perpendicular direction to the incident beam. The quantity of anvil, sample and gasket material the neutrons encounter depends on the precise scattering angle. For all materials in use, absorption

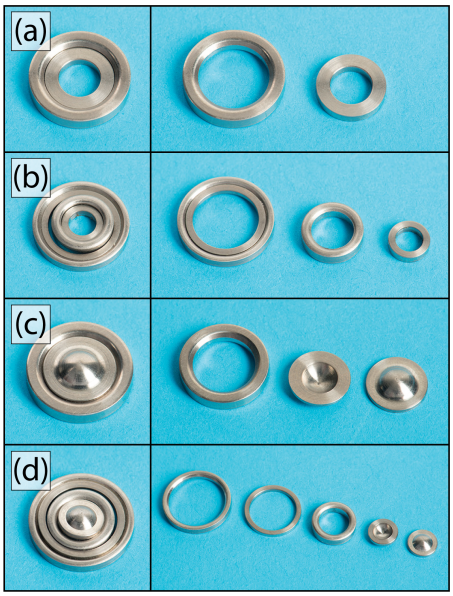

Figure 4. Standard variants of null-scattering Ti–Zr gaskets in current use: (a) single-toroidal, (b) double toroidal, (c) encapsulated single-toroidal and, (d) encapsulated double-toroidal. Sample volumes are approximately 100, 33, 66, and 22 mm^3, respectively.

measurements have been performed and currently these are used within a Monte-Carlo algorithm, developed in-house, that chooses random vectors between the sample space and the detector surface. These randomly-chosen paths are then ray-traced and the extent of beam attenuation, for all wavelengths, is calculated for each individual path—this leads ultimately to a full Monte Carlo-simulated attenuation measurement across the whole detector face and within the whole sample volume. This attenuation factor also changes with increasing applied load as the dimensions of the components vary.

5. Varying temperature under pressure

It is now commonplace to explore the effects of pressure in conjunction with other variables; experiments on PEARL offer the possibility of investigating samples at high- and low-temperatures, while under pressure, aiding study of e.g. hydrogen ordering, magnetism or charting phase space. Currently, the 80–1400 K temperature range is accessible—although the full range cannot be covered in a single experiment—and in this Section we describe the means by which these temperatures are generated.

5.1. *Low temperatures (80–500 K)*

There are two methods used to reach low temperatures—either simply partially immersing the PE press in liquid nitrogen,[24] or by an insert device that flows liquid nitrogen in a more targeted manner, around the anvils. The first approach is arguably the simplest and allows access to the 80–350 K range with an uncertainty of ca. 2 K. The press is first placed within a cradle and then lowered into a liquid-nitrogen-filled cryostat tank consisting of a double-walled, evacuated jacket, with a perspex lid—see Figure 5 for images of the apparatus. As the press is not under vacuum, this approach provides the advantageous ability to access the PE press physically, within the cryostat tank. This direct access allows the recovery of samples to true ambient conditions (by opening the threaded breech manually) whilst in the instrument and has been used to great effect for further investigation

at ambient conditions,[25] and upon extraction for additional characterisation by other methods.

The drawbacks, however, include the strong neutron scattering associated with liquid nitrogen, which reduces detector coverage between ca. 80–100 K (as the liquid partially covers the detector view of the tank), and the difficulty in maintaining an operational piston seal at these low temperatures. The latter point is addressed by using a helium gas-driven, pre-stressed, indium-supported Bridgman seal, which can withstand a maximum applied load of 60 tonnes.[26] If the sample is warmed under a constant hydraulic load, there can be difficulties in maintaining pressure as friction around the seal reduces when temperature increases. The alternative is to replace the helium with a mixture of 5:1 iso-*n*-pentane which remains liquid to ca. 110 K, even at a pressure of 1 kbar.[27] In this instance, a seal made of steel-reinforced polytetrafluoroethylene can be used instead, which does not suffer from loss of friction on warming, thus maintaining a constant pressure. With pentane seals, up to 200 tonnes of applied load can be delivered, limited only by the gasket and anvil geometry. Using a standard Eurotherm controller, the temperature of each anvil is operated independently of the other, which allows for compensation in thermal mass imbalances. This procedure is computer-controlled and can be scripted for automation, within the SECI environment.

The alternative method of sample cooling at pressure is achieved by flowing liquid nitrogen through a set of rings surrounding the toroidal anvils and steel frettage (Figure 5). Temperatures between 110–500 K are possible, with a nominal stability of ±1 K, coupled with pressures of up to 28 GPa. The rate of temperature change, as well as the time taken for thermal equilibration at the sample, are dramatically reduced compared to those in the immersion-based method. The main body of the press is maintained at room temperature by means of a water circulation bath and a thermally-insulating layer of zirconia seat cores between the press and the anvils; room temperature grants the use of oil to drive the piston, which in turn permits controlled pressure changes at all temperatures allowed by the insert device. Eurotherm-controlled, in-built heaters on the anvils are used to warm the sample, tensioning against the cooling power of the liquid nitrogen. The rate of delivery of the nitrogen is controlled by a servo-driven needle valve, and a steady flow to the anvils is ensured by pressurising the nitrogen dewar with a gas bottle and regulating this with an automatic electronic pressure control valve, the effect being that the internal pressure of the dewar is independent of liquid nitrogen volume. As the press is inaccessible during the experiment it is not possible to recover samples to true ambient conditions.

5.2. *High temperatures (above 500 K)*

Temperatures exceeding 500 K are achieved using internal heating setups based on those developed for synchrotron and offline large-volume, multi-anvil techniques that generate high pressure and temperature simultaneously. The general setup used on PEARL utilises resistive heating by a graphite tube contained inside a thermally- and electrically-insulating gasket assembly, which can generate temperature and pressure of 1400 K and 10 GPa, respectively.[28] Heating power is delivered by a Sorensen DC power supply, which is controlled externally by the SECI environment and can be controlled by a script running on the PEARL PC. Currently, there are three anvil designs: a simple toroidal profile, a ‘conoidal’ profile, and anvils with an inner ‘conoidal’ profile with an additional toroid.[2] The toroidal ring provides further support to the gasket increasing the pressure limit achievable. The anvils are held at lower temperatures by an enclosing ring around each, through which cooling water flows. A fail-safe system ensures that the anvil surface temperature cannot rise above 410 K. Similarly to the low-temperature setups, the PE press body is maintained at ca. 290 K by a second water circulation circuit, else the hydraulic

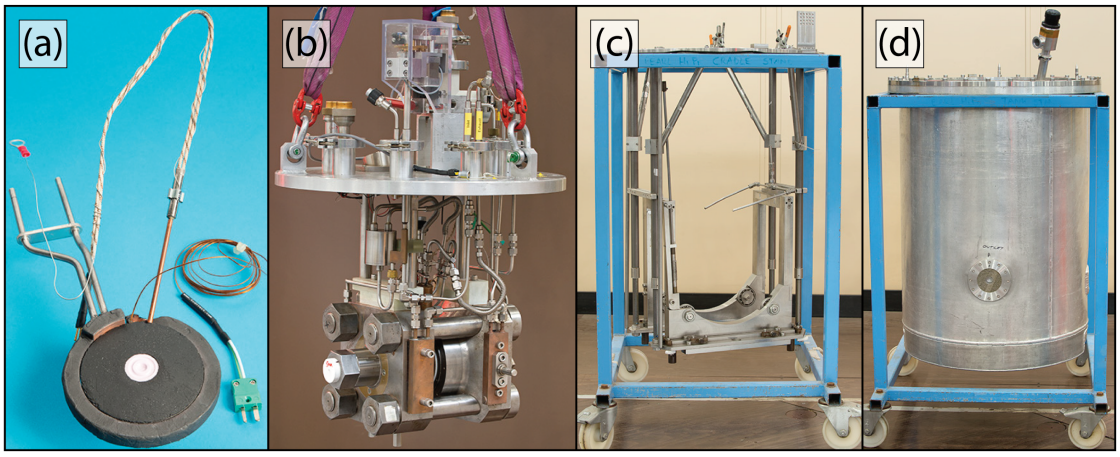

Figure 5. (a) Variable-temperature insert ZTA anvil, located in a liquid nitrogen cooling ring, with a resistive cartridge heater and thermocouple built into the anvil fret. (b) Variable-temperature press, based on the V3 PE press. The visible pipework supplies liquid nitrogen to the cooling rings shown in (a). Nitrogen flow is controlled by a needle valve, located above the mounting flange. The body of the press is maintained at room temperature by flowing water through copper blocks. (c) Cradle in which standard PE press is located prior to being immersed in liquid nitrogen in (d) the cryostat tank. A combination of the cradle and tank, permits an experimental temperature range of 80–370 K and access to the press, allowing sample recovery.

piston seal fails at high press temperatures. The temperature at the sample position is measured with the neutron resonance spectroscopic technique, using thin hafnium and tantalum foils; this is described elsewhere.[29] The resonance energies are measured using downstream monitors (the V4 PE press, has an aperture cut in the rear that allows the transmitted beam to pass through) at the same time as diffraction data are recorded in the transverse detector banks. This technique means that there is no risk of thermocouple failure at high pressures (being broken on compression). Recently, improvements in the signal-to-noise level have been reported by Klotz *et al*, as well as applying it in determination of the triple point of iron.[30]

6. Scientific examples

In this section we provide some brief, representative examples of science that have been performed on the PEARL instrument, spanning a range of disciplines that reflects the interests of the current user community. These examples are not exhaustive of the work performed and published, but act as an illustration of the instrument, its infrastructure, and capabilities.

6.1. *Small molecule structures*

As discussed earlier, one of the key advantages of neutron scattering over X-rays is its ability to identify accurately hydrogen atom positions, when substituted with deuterium. This is particularly pertinent to the field of small, organic systems, where hydrogen atoms are often numerous, constituting a considerable percentage of all atoms in the molecule. On PEARL, some studied examples include members of the amino acid family, where: new phases of L-serine have been identified;[31] a detailed understanding of the thermodynamic stability in ϵ-glycine has been obtained;[32] and pressurisation of L-alanine to 15.5 GPa[33]—using a simultaneous pressure/heating method to maintain hydrostaticity, described by Klotz *et al* [17]—which is one of the highest-pressure crystal structure determinations by neutrons of an organic system; its powder patterns are shown in Fig-

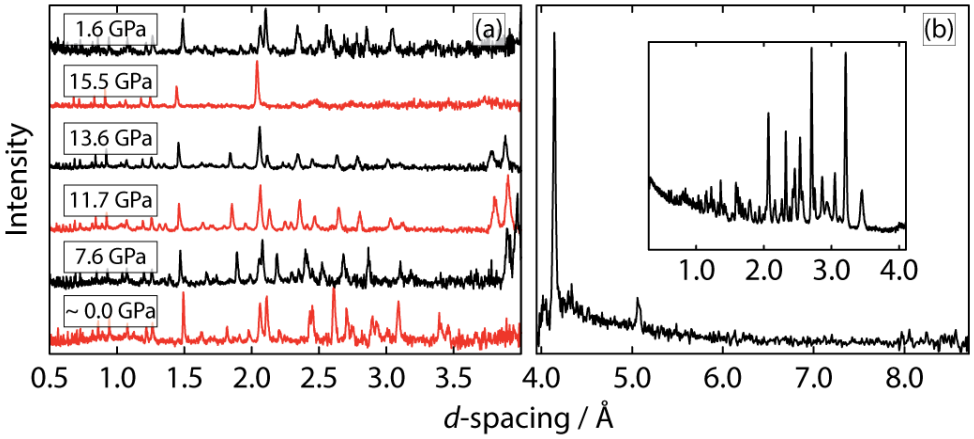

Figure 6. (a) High pressure diffraction pattern of L-alanine using sintered diamond anvils up to 15.5 GPa. Disappearance of the sample peaks at the highest pressure indicates sample amorphisation, driven by the thermodynamic need to minimise volume.[33] The remaining peaks correspond to scattering from the anvils and the pressure marker. Reemergence of the crystalline structure on decompression, measured at 1.6 GPa, demonstrates reversibility of the transition. (b) Long *d*-spacing frame (ToF = 40 ms) of the ammonium bicarbonate diffraction pattern, revealing otherwise unmeasured reflections at ca. 4.2 and 5.1 Å. The inset plot shows the measured diffraction pattern of the same material using the 'standard' 20 ms frame.

ure 6. Further exploiting the hydrogen-discriminating power of neutrons are hydrated molecular systems—high pressure studies led to the identification of a new phase of nitric acid dihydrate and definitive hydrogen-positioning, as well as the observation of isotopic polymorphism, in sodium formate dihydrate.[34, 35] Some more recent experiments have sought to effect structural change not only in the crystal packing, but also at the molecular level; pressure-induced polymerisation was achieved in both acrylic and methacrylic acids.[36, 37] It is becoming more commonplace for pressure experiments to be supported, and complemented by, computational methods; one such study looked at the possibility of proton shift mechanisms controlling the structural configurations of oxalic acid.[38]

6.2. *Fundamental ice physics*

There is a significant body of work investigating the bonding and properties of simple molecular ices such as ND_3 and D_2O. These fundamental physical studies can provide information on the changes in interatomic potentials with increasing pressure. The resolution of the PEARL instrument and its infrastructure have allowed, for example, structure determination of the high pressure phase (IV) of ammonia, showing it to be orthorhombic and not hexagonal, as previously suggested by others.[39] In tetragonal D_2O ice VIII, it was shown that the rate of change in the O–D distance is smaller than that obtained by X-ray diffraction and optical methods, up to 10 GPa, suggesting a decrease in the O-D force constant, given the minimal observable change in the O–D bond distance.[40] In another study, the structure of the disordered ice VII phase revealed multi-site disorder of both the oxygen and deuterium atoms, up to 20 GPa.[41] PEARL has been used to determine a full P–V–T equation of state for ice VI, showing that the hexagonal phase VI of D_2O is 5% stiffer than the H_2O equivalent.[42] The phase behaviour of amorphous D_2O ice has also been explored—providing a deeper understanding of a potential second critical point in the supercooled liquid phase of water at 220 K and 0.1 GPa.[43]

6.3. *Planetary bodies*

The low-temperature and high pressure capabilities, available for the user programme, present the possibility of reproducing the extreme conditions that exist on the surfaces and interiors of planetary bodies and their satellites. This allows us to explore the structures of candidate materials that are expected to occur on these celestial objects. For example, the Pluto New Horizons probe recently identified mixtures of N_2-CO_2-CH_4 ices on the surface of Pluto, and hydrates of ammonia on its moon, Charon.[44] Interactions of these small molecules are expected to form other 'minerals' such as ammonium carbonates. To this end, PEARL has been used recently to study ammonium bicarbonate, which may be present inside Pluto. New phases of this solid material were found at high pressure and low temperature where indexing of these new structures was aided by use of the long fourth pulse sequence provided by the ISIS source, as described in Section 2. Taking advantage of the longer d-spacing reflections from a strongly-scattering sample provides greater certainty in indexing of the unit cell and identification of systematic absences for previously unreported structures.[45] An example diffraction pattern with the long d-spacing reflections is shown in Figure 6. Other planetary ices and related materials include mixtures of ammonia and water,[46, 47] and simple (but structurally complex) high pressure forms of methane;[48] all these studies have made use of the capability to load samples directly into the press whilst at low temperatures. Often these studies, and many others on PEARL, are performed in parallel to equivalent X-ray diffraction experiments and computer simulations.[49] In the high pressure diffraction study of synthetic epsomite ($MgSO_4{\cdot}7H_2O$) ultrasonic measurements provided complementary information relating to the modelling of planetary bodies, in which hydrated sulphate minerals have an important role in rock-formation.[50]

6.4. *High temperatures and Earth sciences*

As alluded to in previous sections, much of the work performed at the extremes of pressure and temperature is on materials with a geological/Earth sciences relevance, such as magnesiowustite $(Mg_{1-x}Fe_x)O$ and $Fe_{0.94}O$, which are fundamental solids in nature.[51, 52] A study of dense liquid water at 6.5 GPa and 670 K performed in conjunction with empirical potential structure refinement (EPSR),[53] showed that the local structure of high-density water is reminiscent of more simple liquids.[54] Brucite $Mg(OD)_2$ has been studied up to 793 K and 5.2 GPa simultaneously, the results of which raised the discussion of a single- versus three-site model for the deuterium positions under these extreme conditions.[29] Investigations have extended to magnetic properties where, in $LaCoO_3$, the response of the spin state transition of the cobalt cation was observed at 3.7 GPa, up to a temperature of 905 K.[55] In situations where the desired pressures and temperatures remain as-yet unreachable—such as the perovskite–post-perovskite transition of $MgSiO_3$ that occurs at 120 GPa and 2500 K—it is possible to study structural analogues of the post-perovskites at lower (yet elevated) pressures, such as the room-temperature structure of $RbCaF_3$, reported by Knight *et al.*[56]

6.5. *Energetic materials*

Energetic materials (explosives, propellants, and gas generators) represent an important, but challenging class of samples, on account of their potential for rapid and explosive decomposition. Significant efforts have been made on the PEARL instrument to enable the safe and routine handling of these materials in the PE press. The information provided by studies of these materials at extreme pressure and temperature is crucial for understand-

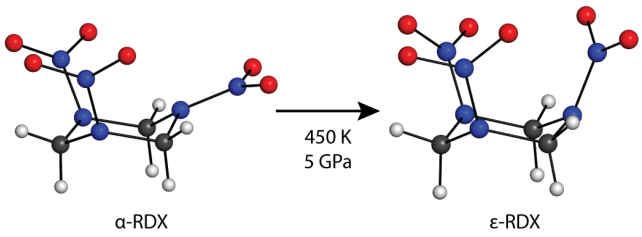

Figure 7. Refined molecular structures of α- and ϵ-RDX. An equatorial $\rightarrow$ axial conformational change in a nitro group accompanies the high pressure, high-temperature transition.[57]

ing and modelling their characteristics and performance under detonation conditions. The application of elevated pressures can also lead to the formation of new polymorphs, and on occasion these are sufficiently metastable that they can be recovered back to ambient pressure. An excellent example is provided by RDX (cyclotrimethylenetrinitramine), a widely-used military explosive that is a major component of many plastic explosive compositions. Using the variable temperature insert it was possible to obtain the high pressure, high-temperature ϵ-form of RDX by compressing the α-form to 5 GPa at 450 K—the molecular structures are shown in Figure 7.[57] On cooling the sample to 150 K, the ϵ-form could be recovered back to ambient pressure, and this phase persisted up to temperatures of 220 K. The ϵ-form was denser than the α-form across the entire pressure range and this is of particular significance as the detonation velocity of an explosive is approximately proportional to the density of the material. Another example is provided by NaN_3 (sodium azide), a material that has been widely used in automotive air bags. Compression of the α-phase to 3.3 GPa at 393 K results in a phase transition to the tetragonal γ-phase, which is isostructural with the azides of the heavier Group 1 elements and features square-antiprism co-ordination of the cations. On decompression at ambient temperature, the γ-phase reverts to the α-phase, but with substantial peak broadening indicative of significant strain within the recovered sample.[58]

6.6. *Disordered materials*

High pressure experiments on PEARL are not limited to powdered crystalline samples; much work has been performed investigating amorphous, liquid or disordered materials. These include extensive studies on the polymorphs and behaviour of amorphous ice phases, where the scattering data on these systems have been modelled using the EPSR methodology.[53, 59] More recently, there has been growing interest in the measurement of high-quality neutron diffraction data from network glasses at very high pressures (ca. 25 GPa). In order to achieve this, diffraction patterns with good statistics that are free of contamination from the gasket and anvil material, are required; this is achieved through very careful setup of the press and anvil configuration, ensuring its reproducibility across all datasets. Some successful examples of these experiments include $MgSiO_3$ and $GeSe_4$.[60, 61] Current capabilities now extend to measuring data from partially disordered crystalline materials and analysing these with the reverse Monte Carlo method.[62, 63]

7. Conclusions

The PEARL instrument is dedicated to high pressure neutron diffraction. In this paper we have described the variable pressure and temperature capabilities that are available to the user programme at ISIS. We are currently able to span the pressure range of 0.5–28 GPa over the temperature range 80–1400 K. The experimental setup is designed to ensure that even inexperienced users of pressure are able to make use of extreme conditions in their

research. Work is ongoing on PEARL to push the pressure and temperature limits even further; a diamond anvil cell project is currently being commissioned, using techniques similar to those at the Oak Ridge Spallation Neutron Source, and is intended to form a part of the user programme in the near-future.[64] This development will not only provide access to higher pressures than currently available, but also all the benefits provided by in-situ optical access to the sample. Other ongoing projects include commissioning of a two-headed CCR system that will cool the anvils to a sub-20 K regime, opening up new areas of physics available on the instrument, and an active development programme to increase the temperature and pressure limit on the broader fields of geologically-relevant materials and materials chemistry.

8. Acknowledgements

This paper is written in memory of William 'Bill' G. Marshall who was the original instrument scientist on the PEARL instrument from 1998 to 2015, and sadly passed away in October 2015. Bill was also a member of the Edinburgh team throughout the construction and commissioning of PEARL from 1994 until 1998.

We gratefully acknowledge the help of Kevin Knight in preparation of the manuscript and contribution in many matters relating to the science programme of PEARL. We also acknowledge the contributions of Richard Nelmes, John Loveday, Rory Wilson, Malcolm Guthrie (University of Edinburgh), the late Michel Besson, Gerard Hamel, Stefan Klotz and Guillaume Weill (UPMC, Paris), and those of the ISIS facility staff: Oleg Kiricheck, Chris Goodway, Mark Kibble, John Dreyer, Andy Chamberlain, Chris Barry, Steve Boon and Chris Ridley. We acknowledge Dominic Fortes, Chris Howard, and Colin Pulham for direct contribution of data in Section 6. Thanks to Simon Waller and Stephen Kill for assistance with images. Funding for the initial design and build of the PEARL instrument was provided by an EPSRC Facility Development Fund and the most recent upgrade of PEARL was funded by the CSIC (Consejo Superior de Investigaciones Científicas) in Spain. We acknowledge the engineering support of Natxo Carrera of AVS, Spain and of Javier Bermejo, Madrid. Finally we acknowledge the contributions of all those referenced within this work and those we have been unable to reference.

References

[1] Guthrie M. Future directions in high-pressure neutron diffraction. J Phys Condens Mat. 2015;27:153201.
[2] Klotz S. Techniques in high pressure neutron scattering. London , UK: CRC Press, Taylor and Francis, Boca Raton; 2013.
[3] McWhan DB, Bloch D, Parisot G. Apparatus for neutron diffraction at high pressure. Rev Sci Inst. 1974;45(5):643–646.
[4] Besson JM, Nelmes RJ, Hamel G, Loveday JS, Weill G, Hull S. Neutron powder diffraction above 10 GPa. Physica B. 1992;180:907–910.
[5] Khovstantsev LG. A verkh-niz (up-down) toriod device for generation of high pressure. High Temp High Press. 1984;16:165–169.
[6] Klotz S, Besson JM, Hamel G, Nelmes RJ, Loveday JS, Marshall WG, Wilson RM. Neutron powder diffraction at pressures beyond 25 GPa. Appl Phys Lett. 1995;66:1735–1737.
[7] Scintacor. 2016; Available from: http://www.scintacor.com/.
[8] Klotz S, Hamel G, Frelat J. A new type of compact large-capacity press for neutron and X-ray scattering. High Press Res. 2004;24:219–223.
[9] Arnold O *et al*. Mantid—Data analysis and visualization package for neutron scattering and μSR experiments. Nucl Instrum Meth A. 2014;764:156–166.

[10] Toby BH. *EXPGUI*, a graphical user interface for *GSAS*. J Appl Crystallogr. 2001;34(2):210–213.
[11] Rodríguez-Carvajal J. Recent advances in magnetic structure determination by neutron powder diffraction. Physica B. 1993;192:55–69.
[12] Coelho A. TOPAS-Academic: General Profile and Structure Analysis Software for Powder Diffraction Data. Version 5.0. Brisbane, Australia; 2012.
[13] Khovstantsev LG, Slesarev VN, Brazhkin VV. Toroid type high-pressure device: history and prospects. High Press Res. 2004;24:371.
[14] Fang J, Bull CL, Loveday JS, Nelmes RJ, Kamanev KV. Strength analysis and optimisation of double-toroidal anvils for high-pressure research. Rev Sci Inst. 2012;83:093902.
[15] Marshall WG, Francis DJ. Attainment of near-hydrostatic compression conditions using the Paris-Edinburgh cell. J Appl Crystallogr. 2002;35:122–125.
[16] Piermarini GJ, Block S, Barnett JD. Hydrostatic limits in liquids and solids to 100 kbar. J Appl Phys. 1973;:5377–5382.
[17] Klotz S, Paumier L, Marchand GL, Munsch P. The effect of temperature on the hydrostatic limit of 4:1 methanol-ethanol under pressure. High Press Res. 2009;29:649–652.
[18] Sidorov VA, Sadykov RA. Hydrostatic limits of fluorinert liquids used for neutron and transport studies at high pressure. J Phys Condens Mat. 2005;17(40):S3005.
[19] Loveday JS, Hamel G, Nelmes RJ, Klotz S, Guthrie M, Besson JM. Neutron diffraction studies of hydrogen-bonded ices at high pressure. High Press Res. 2000;17(3-6):149–155.
[20] Bocian A, Bull CL, Hamidov H, Loveday JS, Nelmes RJ, Kamenev KV. Gas loading apparatus for the Paris-Edinburgh press. Rev Sci Inst. 2010;81(9):093904.
[21] Bull CL, Bocian A, Hamidov H, Kamenev KV, Nelmes RJ, Loveday JS. Note: Achieving quasi-hydrostatic conditions in large-volume toroidal anvils for neutron scattering to pressures of up to 18 GPa. Rev Sci Inst. 2011;82(7):076101.
[22] Klotz S, Philippe J, Bull CL, Loveday JS, Nelmes RJ. A 3 kbar hydrogen-compatible gas loader for Paris–Edinburgh presses. High Press Res. 2013;33(1):214–220.
[23] Wilson RM, Loveday JS, Nelmes RJ, Klotz S, Marshall WG. Attenuation corrections for the Paris-Edinburgh cell. Nucl Inst and Meth A. 1995;354:145.
[24] Klotz S, Besson JM, Hamel G, Nelmes RJ, Loveday JS, Marshall WG. High pressure neutron diffraction using the Paris-Edinburgh cell: Experimental possibilities and future prospects. High Press Res. 1996;14(4-6):249–255.
[25] Klotz S, Besson JM, Hamel G, Nelmes RJ, Loveday JS, Marshall WG. Metastable ice VII at low temperature and ambient pressure. Nature. 1999;398:681–684.
[26] Klotz S, Padmanabhan B, Philippe J, Strässle T. The use of a 'Bridgman-seal' for low-temperature hydraulics. High Press Res. 2008;28:621–625.
[27] Klotz S, Philippe J, Cochard E. Solidification and viscosity of iso-pentane/n-pentane mixtures at low temperatures and high pressure. J Phys: Appl Phys. 2006;39(8):1674.
[28] Zhao Y, Von Dreele RB, Morgan JG. A high P–T cell assembly for neutron diffraction up to 10 GPa and 1500 K. High Press Res. 1999;16(3):161–177.
[29] Le Godec Y, Dove MT, Francis DJ, Kohn SC, Marshall WG, Pawley AR, Price GD, Redfern SAT, Rhodes N, Ross NL, Schofield PF, Schooneveld E, Syfosse G, Tucker MG, Welch MD. Neutron diffraction at simultaneous high temperatures and pressures, with measurement of temperature by neutron radiography. Mineral Mag. 2001;65(6):737–748.
[30] Klotz S, Le Godec Y, Strässle T, Stuhr U. The α–γ–ϵ triple point of iron investigated by high pressure–high temperature neutron scattering. Appl Phys Lett. 2008;93(9):091904.
[31] Moggach SA, Marshall WG, Parsons S. High-pressure neutron diffraction study of L-serine-I and L-serine-II, and the structure of L-serine-III at 8.1 GPa. Acta Crystallogr B. 2006; 62:815–825.
[32] Moggach SA, Marshall WG, Rogers DM, Parsons S. How focussing on hydrogen bonding interactions in amino acids can miss the bigger picture: a high-pressure neutron powder diffraction study of ϵ-glycine. CrystEngComm. 2015;17:5315–5328.
[33] Funnell NP, Marshall WG, Parsons S. Alanine at 13.6 GPa and its pressure-induced amorphisation at 15 GPa. CrystEngComm. 2011;13:5841–5848.
[34] Walker M, Pulham CR, Morrison CA, Allan DR, Marshall WG. Nitric acid dihydrate at ambient and high pressure: an experimental and computational study. Phys Rev B. 2006;

73:224110.
[35] Walker M, Morrison CA, Allan DR, Pulham CR, Marshall WG. A new high pressure phase of sodium formate dihydrate; an experimental and computational study. Dalton Trans. 2007; :2014–2019.
[36] Marshall WG, Urquhart AJ, Owsald IDH. Investigation of methacrylic acid at high pressure using neutron diffraction. J Phys Chem B. 2015;119:12147–12154.
[37] Johnston BF, Marshall WG, Parsons S, Urquhart AJ, Oswald IDH. Investigation of acrylic acid at high pressure using neutron diffraction. J Phys Chem B. 2014;118:4044–4051.
[38] Macchi P, Casati N, Marshall WG, Sironi A. The α and β forms of oxalic acid di-hydrate at high pressure: a theoretical simulation and a neutron diffraction study. CrystEngComm. 2010;12:2596–2603.
[39] Loveday JS, Nelmes RJ, Marshall WG, Besson JM, Klotz S, Hamel G. Structure of deuterated ammonia IV. Phys Rev Lett. 1996;76:74–77.
[40] Nelmes RJ, Loveday JS, Wilson RM, Besson JM, Pruzan P, Klotz S, Hamel G, Hull S. Neutron diffraction study of the structure of deuterated ice VIII to 10 GPa. Phys Rev Lett. 1993;71:1192–1195.
[41] Nelmes RJ, Loveday JS, Marshall WG, Hamel G, Besson JM, Klotz S. Multisite disordered structure of ice VII to 20 GPa. Phys Rev Lett. 1998;81:2719–2722.
[42] Fortes AD, Wood IG, Tucker MG, Marshall WG. The P–V–T equation of state of D_2O ice VI determined by neutron powder diffraction in the range $0 < P < 2.6$ GPa and $120 < T < 330$ K, and the isothermal equation of state of D_2O ice VII from 2 to 7 GPa at room temperature. J Appl Crystallogr. 2012;45(3):523–534.
[43] Nelmes RJ, Loveday JS, Strässle T, Bull CL, Guthrie M, Hamel G, Klotz S. Annealed high-density amorphous ice under pressure. Nature Phys. 2006;2.
[44] Grundy WM *et al*. Surface compositions across Pluto and Charon. Science. 2016; 351(6279):aad9189.
[45] Howard C, Fortes A. In preparation. 2016;.
[46] Loveday JS, Nelmes RJ, Bull CL, Maynard-Casely HE, Guthrie M. Observation of ammonia dihydrate in the AMH-VI structure at room temperature—possible implications for the outer solar system. High Press Res. 2009;29(3):396–404.
[47] Fortes AD, Wood IG, Vočadlo L, Knight KS, Marshall WG, Tucker MG, Fernandez-Alonso F. Phase behaviour and thermoelastic properties of perdeuterated ammonia hydrate and ice polymorphs from 0 to 2 GPa. J Appl Crystallogr. 2009;42(5):846–866.
[48] Maynard-Casely HE, Bull CL, Guthrie M, Loa I, McMahon MI, Gregoryanz E, Nelmes RJ, Loveday JS. The distorted close-packed crystal structure of methane A. J Chem Phys. 2010; 133(6):064504.
[49] Wilson CW, Bull CL, Stinton G, Loveday JS. ????;.
[50] Gromnitskaya EL, Yagafarov OF, Lyapin AG, Brazhkin VV, Wood IG, Tucker MG, Fortes AD. The high-pressure phase diagram of synthetic epsomite ($MgSO_4 \cdot 7H_2O$ and $MgSO_4 \cdot 7D_2O$) from ultrasonic and neutron powder diffraction measurements. Phys Chem Miner. 2013;40(3):271–285.
[51] Wood IG, Vocadlo L, Dobson DP, Price D, Fortes AD, Cooper FJ, Neale JW, Walker AM, Marshall WG, Tucker MG, Francis DJ, Stone HJ, McCammon CA. Thermoelastic properties of magnesiowustite, $(Mg_{1-x}Fe_x)O$: determination of the Anderson– Grüneisen parameter by time-of-flight neutron powder diffraction at simultaneous high pressures and temperatures. J Appl Crystallogr. 2008;41:886–896.
[52] Klotz S. Neutron diffraction studies on "simple" iron oxides under pressure: Fe_3O_4, α-Fe_2O_3, and FeO. Chin Sci Bull. 2014;:5241–5250.
[53] Soper AK. Partial structure factors from disordered materials diffraction data: An approach using empirical potential structure refinement. Phys Rev B. 2005;72:104204.
[54] Strässle T, Saitta AM, Godec YL, Hamel G, Klotz S, Loveday JS, Nelmes RJ. Structure of dense liquid water by neutron scattering to 6.5 GPa and 670 K. Phys Rev Lett. 2006; 96:067801.
[55] Kozlenko DP, Golosova NO, Jirák Z, Dubrovinsky LS, Savenko BN, Tucker MG. Temperature- and pressure-driven spin-state transitions in $LaCoO_3$. Phys Rev B. 2007; 75:064422.

[56] Knight KS, Marshall WG, Hawkins PM. A high-pressure neutron diffraction study of the ferroelastic phase transition in $RbCaF_3$. Phys Chem Miner. 2014;41:461–472.
[57] Millar DIA, Oswald IDH, Barry C, Francis DJ, Marshall WG, Pulham CR, Cumming AS. Pressure-cooking of explosives—the crystal structure of ϵ-RDX as determined by X-ray and neutron diffraction. Chem Commun. 2010;46:5662–5664.
[58] Pulham CR, Millar DIA, Barry C, Marshall WG. Structural characterization of sodium azide and sodium bifluoride at high pressures. Z Kristallogr. 2014;229:259–275.
[59] Klotz S, Hamel G, Loveday JS, Nelmes RJ, Guthrie M, Soper AK. Structure of high-density amorphous ice under pressure. Phys Rev Lett. 2002;89:285502.
[60] Wilding M, Guthrie M, Bull CL, Tucker MG, McMillan PF. Feasibility of in situ neutron diffraction studies of non-crystalline silicates up to pressures of 25 GPa. J Phys Condens Mat. 2008;20(24):244122.
[61] Bouzid A, Pizzey KJ, Zeidler A, Ori G, Boero M, Massobrio C, Klotz S, Fischer HE, Bull CL, Salmon PS. Pressure-induced structural changes in the network-forming isostatic glass $GeSe_4$: An investigation by neutron diffraction and first-principles molecular dynamics. Phys Rev B. 2016 Jan;93:014202.
[62] Tucker MG, Keen DA, Dove MT, Goodwin AL, Hui Q. RMCProfile: reverse Monte Carlo for polycrystalline materials. J Phys Condens Mat. 2007 Jul;19:335218.
[63] Playford HY, Tucker MG, Bull CL. Neutron total scattering of crystalline materials in the gigapascal regime. J Appl Crystallogr. 2016;:Submitted.
[64] Boehler R, Guthrie M, Molaison JJ, dos Santos AM, Sinogeikin S, Machida S, Pradhan N, Tulk C. Large-volume diamond cells for neutron diffraction above 90 GPa. High Press Res. 2013;33(3):546–554.